Fluid Dynamics, Vol. 41, No. 6, 2006, pp. 881–890. Translated from Izvestiya Rossiiskoi Academii Nauk, Mekhanika Zhidkosti i Gaza, No. 6, 2006, pp. 29–39.

Two-Dimensional Problem of Natural Convection in a Rectangular Domain with Local Heating and Heat-Conducting Boundaries of Finite Thickness

G. V. Kuznetsov and M. A. Sheremet

Received June 6, 2005

Abstract — Time-dependent natural convective heat transfer in a closed rectangular domain with heat-conducting boundaries of finite thickness is investigated numerically in the case of local heating on the inner side of the vertical wall. Convection-radiation heat transfer takes place on one of the outer boundaries of the solution domain. The inhomogeneous temperature distribution in the gas cavity is clearly manifested when the Grashof number $\mathrm{Gr} > 10^6$. Circulation flows can be distinguished in various zones of the solution domain on the basis of the numerical investigations carried out. These flows are due to the effect of the heat-release source, the propagation of perturbations induced by elements of the rigid wall, and the dynamics of conductive heat transfer in the solid material. The scales of the effect of the Grashof number on the hydrodynamic and thermal characteristics are indicated.

Keywords: time-dependent natural convective heat transfer, closed rectangular domain, heat-conducting rigid walls, local heat-release source.

The combined analysis of the thermogravitational convection in a cavity occupied by a gas or liquid and the conductive heat transfer in the solid walls around the cavity is of practical interest in different area of technology (gas turbines, design of vehicle fuel systems, heat exchangers, etc.) [1–5].

A few solutions of such problems are known [6–15]. The heat transfer processes have been simulated numerically in the axisymmetric formulation but only for a one-dimensional time-dependent heat conduction equation in the solid phase [6, 7]. It has been found that free cavity convection leads to an intensification of heat removal to the walls [8]. The boundary conditions of the IV-th kind for the energy equation (equality of the temperatures and heat fluxes on the interface between the two media) on all the internal boundaries significantly affect the heat transfer during free cavity convection [8, 9]. For example, the rigid boundary walls affect the conditions of free convection generation in a closed domain [10, 11]. In [12] the free convection in a cavity with one-dimensional heat-conducting and radiating walls was analyzed numerically. Investigations [13, 14] were devoted to the study of the effect of the thickness and thermal conductivity of the transverse walls on the heat emission in free convection in inclined rectangular cavities for the purpose of estimating the efficiency of using cellular structures for reducing the convective heat losses in flat-plate solar collectors. In [15] the effect of the wall thermal conductivity on the free convection in a two-dimensional rectangular cavity was analyzed.

However, in these problems the effect of a heat-release source located in the working cavity and the nonlinear action of the surrounding medium were not considered simultaneously. In particular, this situation can arise in forced-cooling systems for electronic equipment, in hazardous-freight transport containers, in rooms used for social or industrial purposes, etc. The aim of the present study is to simulate mathematically, with allowance for the mechanisms of conduction and natural convection, time-dependent heat transfer in a closed rectangular domain with a locally concentrated heat-release source and inhomogeneous boundary conditions.

0015–4628/06/4106–0881

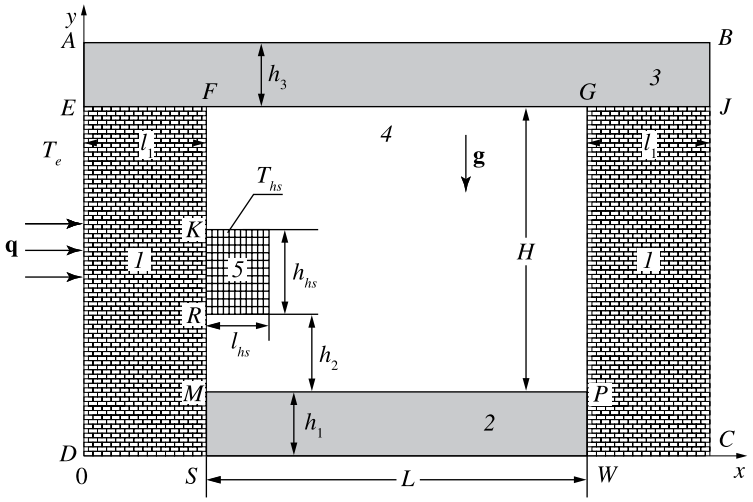

Fig. 1. Solution domain: elements of the solid phase (*1*, *2*, and *3*), gas phase (*4*), heat-release source (*5*)

1. FORMULATION OF THE PROBLEM AND METHOD OF SOLUTION

We will consider the heat transfer process in the domain represented in Fig. 1. The solution domain includes five rectangles of different sizes, similar in shape but with different thermal characteristics. The length of the gas cavity is equal to L and the height to H. We introduce the following Cartesian coordinate system: the origin coincides with the left lower corner of the solution domain. A heat-release source of length l_{hs} and height h_{hs} is located on the inner side of one of the walls. The distance from the base of the solution domain, which represents a subdomain of the solid phase, to the heat-release source is equal to h_2. The initial temperature is constant and equal to T_0 over the entire solution domain, except for the heat-release source. The heat-release source is assumed to have an always constant temperature T_0. The horizontal walls of finite thickness ($y = 0$, $y = h_1 + H + h_3$) and the vertical wall ($x = 2l_1 + L$) which form the cavity were considered to be adiabatic from the outside. Convective-radiative heat transfer with the surrounding medium was taken into account on the wall $x = 0$.

In order to describe the flow and temperature fields in the gas phase we used the time-dependent two-dimensional convection equations in the Boussinesq approximation [16–21] while in the solid phase we considered the two-dimensional heat conduction equation [22, 23].

As the scale of the distance, we took the length of the gas cavity L. As the "velocity vorticity-stream function-temperature" dimensionless variables, we took, respectively,

$$X = \frac{x}{L}, \qquad Y = \frac{y}{L}, \qquad \tau = \frac{t}{t_0}, \qquad U = \frac{u}{V_0}, \qquad V = \frac{v}{V_0}, \qquad \Theta = \frac{T - T_0}{\Delta T}$$

$$\Delta T = T_{hs} - T_0, \qquad V_0 = \sqrt{g\beta\Delta T L}$$

where β is the thermal volume expansion coefficient, t is time, t_0 is the time scale, u and v are the velocity components in projection on the x and y axes, respectively, V_0 is the velocity scale (convection velocity), T is the temperature, T_0 is the temperature of the surrounding medium, and g is the acceleration of free fall.

For the gas phase the dimensionless Boussinesq equations can be written as follows:

$$\frac{1}{\mathrm{Ho}}\frac{\partial\Omega}{\partial\tau} + U\frac{\partial\Omega}{\partial X} + V\frac{\partial\Omega}{\partial Y} = \frac{1}{\sqrt{\mathrm{Gr}}}\Delta\Omega + \frac{1}{2}\frac{\partial\Theta}{\partial X} \tag{1.1}$$

$$\Delta\Psi = -2\Omega \tag{1.2}$$

$$\frac{1}{\mathrm{Ho}}\frac{\partial\Theta}{\partial\tau} + U\frac{\partial\Theta}{\partial X} + V\frac{\partial\Theta}{\partial Y} = \frac{1}{\mathrm{Pr}\sqrt{\mathrm{Gr}}}\Delta\Theta \tag{1.3}$$

where

$$\mathrm{Ho} = \frac{V_0 t_0}{L}, \qquad \mathrm{Gr} = \frac{\beta g L^3 (T_{hs} - T_0)}{\nu^2}, \qquad \mathrm{Pr} = \frac{\nu}{a}$$

For the solid phase the heat conduction equation has the form:

$$\frac{\partial \Theta_i}{\partial \mathrm{Fo}_i} = \Delta \Theta_i, \qquad i = 1, 2, 3 \qquad \mathrm{Fo}_i = \frac{a_i t_0}{L^2} \tag{1.4}$$

Here, Ho is the homochronicity number, Gr is the Grashof number, ν is the kinematic viscosity coefficient, Ω is the vorticity, Ψ is the stream function, Pr is the Prandtl number, a_i is the thermal diffusivity of the ith subdomain, and Fo_i is the Fourier number corresponding to the ith subdomain.

For the system of equations (1.1)–(1.4) the dimensionless boundary conditions have the form:

$$(X, Y) \in AD$$

$$\frac{\partial \Theta_i(X, Y, \tau)}{\partial X} = \mathrm{Bi}_i \Theta_i(X, Y, \tau) + \mathrm{Bi}_i \frac{T_0 - T_e}{T_{hs} - T_0} + Q$$

$$Q = \mathrm{N}_i \left[\left(\Theta_i(X, Y, \tau) + \frac{T_0}{T_{hs} - T_0} \right)^4 - \left(\frac{T_e}{T_{hs}} - T_0 \right)^4 \right], \qquad i = 1, 3$$

$$\mathrm{Bi}_i = \frac{\alpha L}{\lambda_i}, \qquad \mathrm{N}_i = \frac{\varepsilon \sigma L (T_{hs} - T_0)^3}{\lambda_i}$$

$$(X, Y) \in AB \cup BC \cup CD$$

$$\frac{\partial \Theta_i(X, Y, \tau)}{\partial X^k} = 0, \quad i = 1, \ldots, 3; \quad k = 1, 2; \quad X^1 \equiv X, \quad X^2 \equiv Y$$

$$(X, Y) \in EJ \cup FK \cup RS \cup GW \cup MP$$

$$\Theta_i = \Theta_j; \quad \frac{\partial \Theta_i}{\partial X^k} = \lambda_{j,i} \frac{\partial \Theta_j}{\partial X^k}, \quad i = 1, \ldots, 4; \quad j = 1, \ldots, 4; \quad k = 1, 2$$

$$(X, Y) \in FK \cup RM \cup GP \qquad (k = 1, \quad i = 1)$$

$$(X, Y) \in FG \cup MP \quad (k = 2, \quad i = 2, 3)$$

$$\Psi = 0, \qquad \frac{\partial \Psi}{\partial X^k} = 0, \qquad \Theta_i = \Theta_4; \qquad \frac{\partial \Theta_i}{\partial X^k} = \lambda_{4,i} \frac{\partial \Theta_4}{\partial X^k}$$

Here, Bi_i is the Biot number corresponding to the ith subdomain; α is the coefficient of heat transfer between the external medium and the solution domain considered; N_i is the number characterizing the ratio of the heat fluxes due to radiation to the heat fluxes due to conduction corresponding to the ith subdomain; ε is the reduced emissivity; α is the Stefan-Boltzmann constant; $\lambda_{ij} = \lambda_i / \lambda_j$ is the relative thermal conductivity coefficient; and λ_i is the thermal conductivity coefficient of the ith subdomain.

Equations (1.1)–(1.4) were solved by a finite-difference method [24] on a uniform grid using an implicit two-layer scheme.

In order to approximate the convective terms in the evolutionary equations we used the Samarskii monotonic scheme [24]. The value of the vorticity on the boundary was determined from the Woods formula [25]. For solving Eqs. (1.1) numerically, (1.2) we used a finite-difference scheme constructed by analogy with the well-known variable-direction scheme proposed in [26, 27] for solving the heat conduction equation. In this scheme the solution of the two-dimensional system reduces to the successive solution of one-dimensional systems by means of the sweep method [24] as systems of finite-difference equations with three-diagonal matrices. Equations (1.3), (1.4) were solved using the Samarskii locally one-dimensional scheme [24], a simple iteration method being used for solving the nonlinear boundary condition of the IIIrd kind.

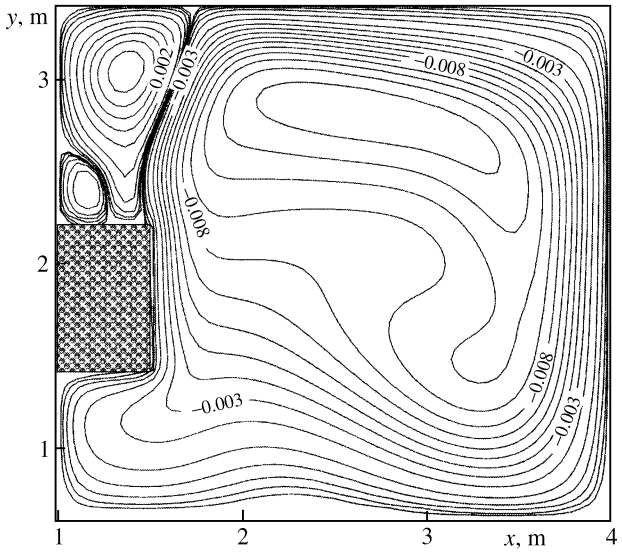

Fig. 2. Streamlines for $\mathrm{Gr} = 10^7$

The variable-direction method used and the locally one-dimensional scheme are absolutely stable and the order of approximation of the input differential problem by the finite-difference scheme is $O(\tau + h^2 + l^2)$ [24].

The Poisson equation (1.2) for the stream function was solved in each time step by the stabilization method [25].

2. DISCUSSION OF THE RESULTS

The investigations were carried out for the following values of the dimensionless parameters: $\mathrm{Ho} = 1$, $\mathrm{Gr} = 10^7$–10^9, and $\mathrm{Pr} = 0.71$, and the determining temperatures $T_e = 253$ K, $T_{hs} = 333$ K, and $T_0 = 293$ K. The numerical analysis was carried out using a uniform 200×200 grid for the following geometric parameters (Fig. 1): $l_1 = 1.0$ m, $l_{hs} = 0.5$ m, $L = 3.0$ m, $h_1 = 0.6$ m, $h_2 = 0.8$ m, $h_{hs} = 0.8$ m, $h_3 = 0.6$ m, and $H = 2.8$ m. Since we considered the essentially time-dependent process $\mathrm{Ho} = 1$, the expression $t_0 = L/V_0 = \sqrt{L/g\beta\Delta T}$ was used for determining the time scale. The hydrodynamic and thermal parameter distributions presented correspond to the instant of time $t = 24$ h.

The heat-release source results in the development of three circulating flows (Fig. 2). In the largest eddy located at the center of the cavity the air moves along closed curves, ascending in the neighborhood of the heat-release source and descending in the neighborhood of the opposite wall. In the gas cavity there are two other small-scale eddies above the heat-release source whose development is attributable to the finite size of the source. The domain above the source can be regarded as a zone in which one of the walls has the maximum temperature. As can be seen from Fig. 2, masses of the gas phase descend along the cold wall and ascend on the side of the central eddy.

The vorticity isoline distribution clearly shows the propagation of perturbations initiated by the wall and the heat-release source into the interior of the air cavity (Fig. 3*a*). The eddies are most intensively formed in the neighborhood of the heat-release source. This is attributable to the intensification of the transfer processes in the neighborhood of the heated section.

The temperature distribution (Fig. 3*b*) demonstrates the effect of the lift force $\rho g\beta(T_{hs} - T_0)$ which develops as a result of the inhomogeneity of the temperature field. In the gas medium the temperature is fairly nonuniformly distributed as a result of the effect of the buoyancy force. The heat-release source also affects the temperature distribution in the rectangle next to which it is located. The domain in question having inhomogeneous thermophysical characteristics, is should be noted that, as the distance from the base decreases, the isotherms become aligned on the interface between the two media.

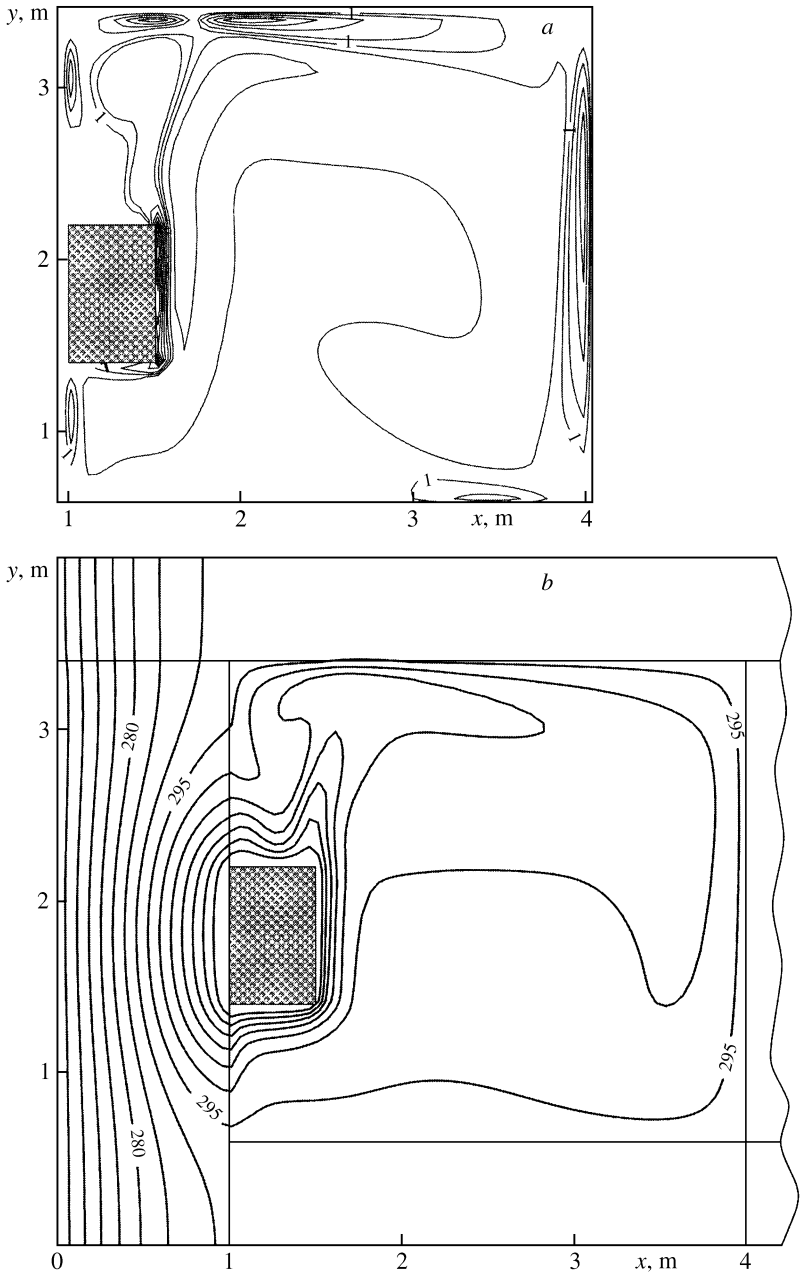

Fig. 3. Fields of the vorticity vector (*a*) and temperature (*b*) for $\mathrm{Gr} = 10^7$ (isotherms are shown in steps of 5 K)

The internal friction forces impede the perturbations departing from the walls. Conversely, the body forces intensify the flow disorder. Consequently, the viscous friction and body forces oppositely affect the flow. In the domain considered the nature of the motion is related with the numerical value of the Gr number. A change in the nature of the motion results in a change in the mechanism of momentum and heat transfer.

The fields of the unknown quantities were obtained in the free-convection flow regime corresponding to $\mathrm{Gr} = 10^8$. As the Grashof number increases from 10^7 to 10^8, the flow structure is observed to change significantly (Fig. 4*a*). The central eddy is unstable and breaks down into smaller-scale eddies. A secondary low-intensity flow develops in the base zone as a result of the effect of the perturbations induced by the solid phase. The temperature field (Fig. 4*b*) changes appreciably; as Gr increases, the heating of the gas phase becomes more intense. This is reflected in the location of the isotherm corresponding to 300 K. In the region above the heat-release source the nonmonotonic isotherm structure is clearer than in Fig. 3*b*. The intense

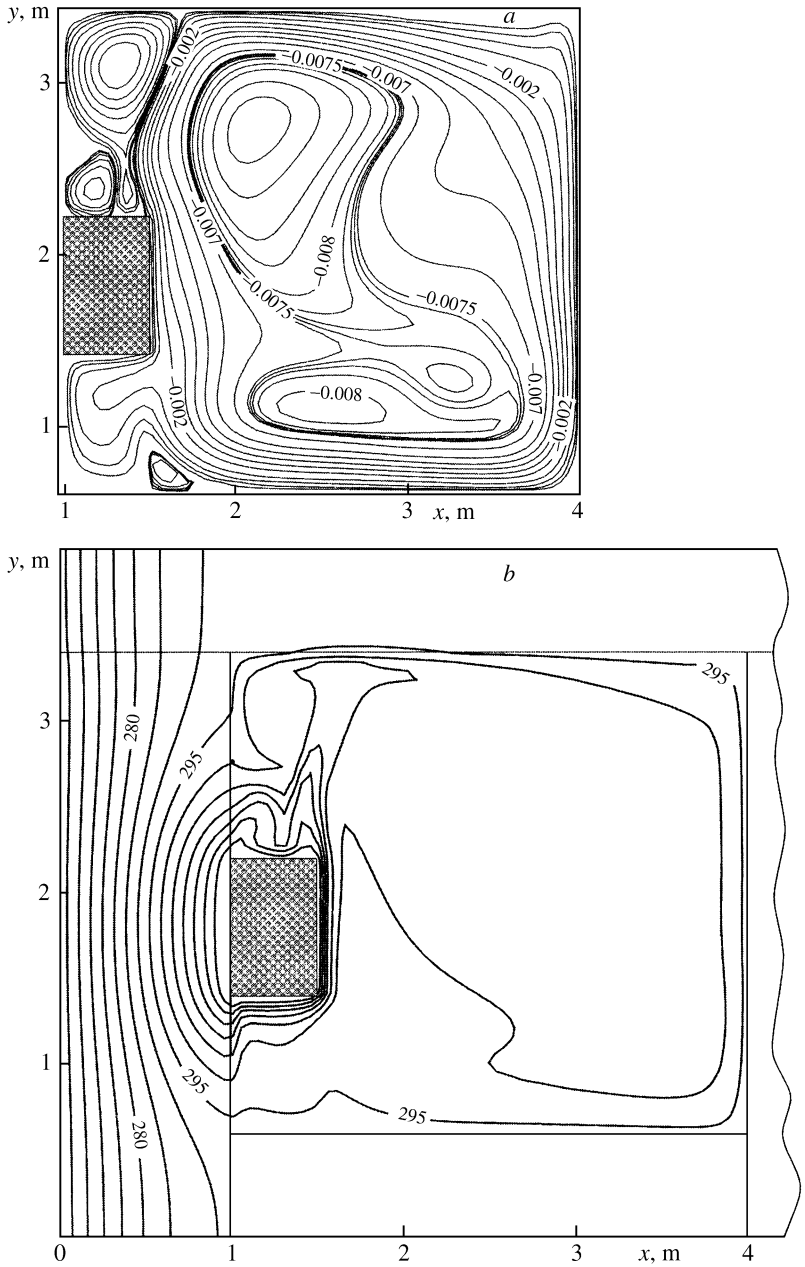

Fig. 4. Streamlines (*a*) and temperature field (*b*) for $\mathrm{Gr} = 10^8$ (isotherms are shown in steps of 5 K)

free-convection flow can lead to intensification of the conductive heat transfer in the solid phase [8]. The calculation results (Fig. 4*b*) confirm this. Thus, a displacement of the isotherm corresponding to 295 K into the interior of the solid phase can be observed on the interface between the solid and gas phases above the heat-release source. In the $\mathrm{Gr} = 10^7$ regime a similar isotherm distribution was not observed. This proves that the heat transfer processes in the gas phase and in the wall elements are essentially interrelated.

In the $\mathrm{Gr} = 10^9$ flow regime the dimensions of the eddy above the heat-release source increase and the eddy envelops the upper gas-phase region (Fig. 5*a*). There is a marked increase in the dimensions of the region corresponding to the secondary flow in the zone above the heat-release source. This is reflected in the temperature distribution (Fig. 5*b*). The eddy on the interface between the base and the gas cavity disappears. In this case a secondary flow similar to the vanished eddy develops on the same interface but displaced toward the right corner. The structure of the central circulating motion changes, the fragmentation disappears, and the eddy structure becomes more integral.

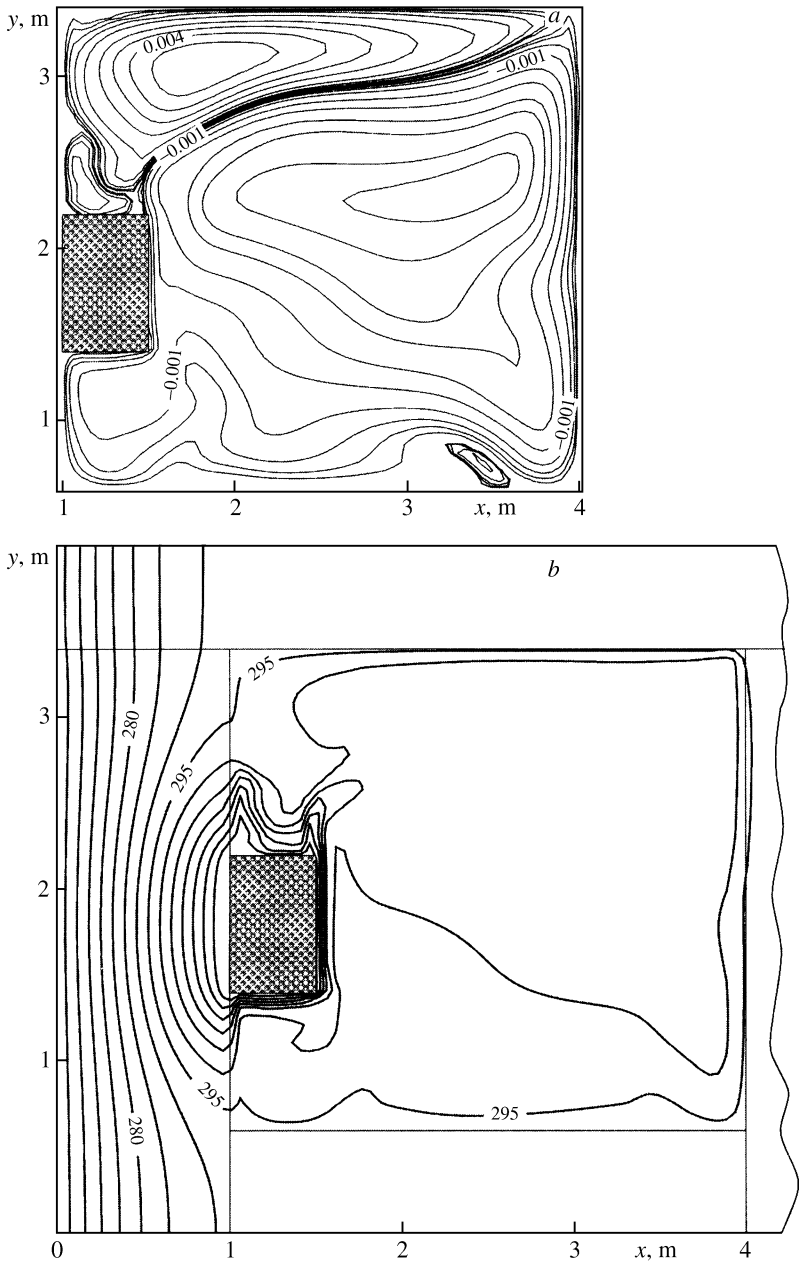

Fig. 5. Same as in Fig. 4 for $\mathrm{Gr} = 10^9$

The temperature is appreciably redistributed (Fig. 5*b*). The dimensions of the higher-temperature zone (the boundary is the 300 K isotherm) decrease as compared with the case $\mathrm{Gr} = 10^8$. The region enveloped by the isotherm corresponding to 305 K also decreases in size. The zone of conductive heat transfer in the solid phase above the heat-release source decreases as compared with it in Fig. 4*b*, while the conductive heat transfer in the wall element located to the right of the source is intensified. The intense heat transfer region is displaced toward the left upper corner of the heat-release source.

We considered the effect of Gr on the temperature distribution along the solution domain in three characteristic cross-sections, namely, below the heat-release source, through the source, and above the source.

When $\mathrm{Gr} = 10^8$ the maximum temperature below the source is reached on the interval $1.8 < x < 4.0$ (Fig. 6*a*). In this case in the zone close to the heat-release source $1.2 < x < 1.8$ the maximum temperature corresponds to the $\mathrm{Gr} = 10^9$ regime. The high temperature gradient on the interface between the solid and

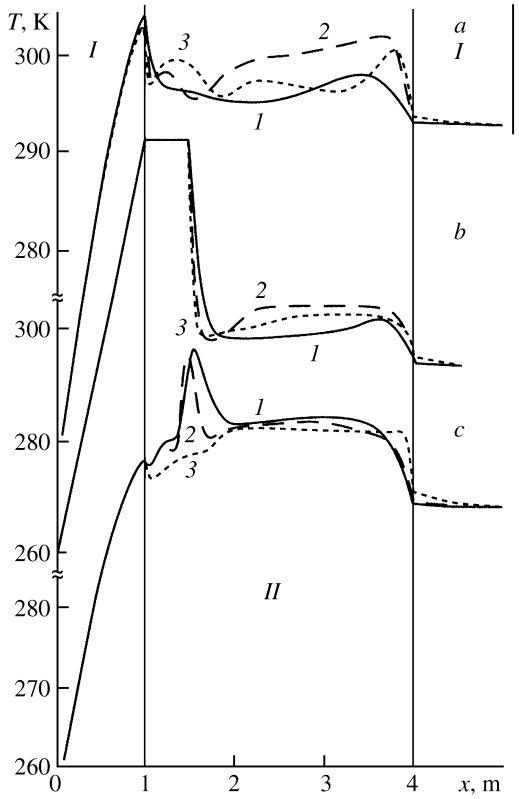

Fig. 6. Temperature distribution in cross-sections passing below the heat-release source (*a*) ($y = 1.0$ m), through the source (*b*) ($y = 1.8$ m), and above the source (*c*) ($y = 2.8$ m) for $\mathrm{Gr} = 10^7$, 10^8, and 10^9 (curves *1–3*, respectively), *I* and *II* correspond to the solid wall and the gas cavity, respectively

gas phases ($x = 1.0$ m) is attributable to the fact that in the solid phase the temperature is fairly uniformly distributed, whereas in the gas phase the heat transfer process is intensified in the region above the heat-release source as a result of the significant effect of the lift force.

In the cross-section passing through the heat-release source in the heater region on the interval $1.5 < x < 1.8$ the maximum temperature corresponds to the $\mathrm{Gr} = 10^7$ regime (Fig. 6*b*). In the direction toward the interior of the gas phase the maximum temperature corresponds to the $\mathrm{Gr} = 10^8$ regime.

In each regime the temperature (Fig. 6*c*) has a fairly nonmonotonic profile. This is attributable to the strong effect of the lift force.

The numerical analysis showed that the free-convection flow regime corresponding to $\mathrm{Gr} = 10^9$ differs qualitatively from the other regimes. For these Grashof numbers the temperature field formed is almost uniform in the upper half of the solution domain. This is due to the fact that the flow and heat transfer are stabilized at a certain level of intensity of the processes of heat transfer from the source and heat removal through the outer boundaries. In this case the localization and boundedness of the source are only slightly reflected in the temperature field of most of the solution domain. A comparison of these results with the characteristics of the heat transfer processes corresponding to the regimes of relatively low Gr (Figs. 2 and 3) shows that intensification of the local heat release leads to a rather non-obvious result. Instead of an increase in the number of vortex structures due to their disintegration with increase in Gr and the corresponding change in temperature distribution, a certain stabilization of the flow and heat transfer is realized due to the effect of the power-consuming condensed phase.

Summary. Heat transfer in a closed rectangular domain is investigated numerically with allowance for heat exchange with the outer medium at Grashof numbers equal to 10^7, 10^8, and 10^9 in the presence of an internal finite-dimension heat-release source and walls of finite thickness with different thermophysical characteristics. As a result of the effect of free convection, an intensification of the heat transfer in the solid

phase is observed at $Gr = 10^8$ and 10^9 (in the solid phase the temperature increases by 2 K). As the Gr number increases, both the scales and the location of the zone of intensification of the heat transfer processes change. At $Gr = 10^9$ the temperature is more uniformly distributed over the entire cavity as compared with $Gr = 10^7$ and 10^8. This indicates a change in the flow regime. At greater Gr the flow and heat transfer are stabilized due to the effect of the power-consuming condensed phase which is capable of accumulating the energy in amounts hundreds of times greater than the source heat release.

The work was carried out with financial support from the Russian Foundation for Basic Research and the Administration of the Tomsk region (project No. 05-02-98006 competition r_ob'_a).

REFERENCES

1. V. G. Gorobets, "Conjugate heat transfer of vertical surfaces with continuous ribbing under natural convection," *Izv. RAN. Energetika*, No. 3, 132–140 (2003).
2. B. B. Petrikevich, S. D. Panin, and A. V. Astrakhov, "Use of the integral boundary layer theory for solving conjugate heat transfer problems for high-energy apparatus channels," *Inzh.-Fiz. Zh.*, **73**, No. 1, 131–137 (2000).
3. A. V. Lykov, V. A. Aleksashenko, and A. A. Aleksashenko, *Conjugate Problems of Convective Heat Transfer* [in Russian], Belorussian University Press, Minsk (1971).
4. M. V. Makarov and G. G. Yan'kov, "Numerical investigation of heat- and mass-transfer processes in a cryogenic fuel tank," in: *Proceedings of 3rd Ros. Nat. Conf. on Heat Transfer*, Vol. 3 [in Russian], Moscow Energy Institute Press, Moscow (2002), pp. 102–107.
5. V. S. Berdnikov, V. V. Vinokurov, V. I. Panchenko, and S. V. Solov'ev, "Heat transfer in the classical Czochralski method," *Inzh.-Fiz. Zh.*, **74**, No. 4, 122–127 (2001).
6. L. A. Moiseeva and S. G. Cherkasov, "Natural convection and heat transfer in a cylindrical vessel for a distributed heat supply and in the presence of local heat sinks on the wall," in: *Proceedings of 2nd Ros. Nat. Conf. on Heat Transfer*, Vol. 3 [in Russian], Moscow Energy Institute Press, Moscow (2002), pp. 108–111.
7. L. A. Moiseeva and S. G. Cherkasov, "Theoretical investigation of the quasi-steady regime of natural convection in a vertical cylindrical vessel with a heat-conducting wall," in: *Proceedings of 3rd Ros. Nat. Conf. on Heat Transfer*, Vol. 3 [in Russian], Moscow Energy Institute Press, Moscow (2002), pp. 116–119.
8. S. M. El-Sherbiny, K. G. T. Hollands, and G. D. Raithby, "Effect of thermal boundary conditions on natural convection in vertical and inclined air layers," *Trans. ASME. C. J. Heat and Mass Transfer*, **104**, No. 3, 515–520 (1982).
9. I. Catton, "Natural convection in enclosures," in: *Proc. 6th Intern. Heat Transfer Conf., Toronto*, Vol. 6, Hemisphere, Washington, D. C. (1978), pp. 13–31.
10. I. Catton, "The effect of insulating vertical walls on the onset of motion in a fluid heated from below," *Intern. J. Heat and Mass Transfer*, **15**, No. 4, 665–672 (1972).
11. D. M. Kim and R. Viskanta, "Effect of wall heat conduction on natural convection heat transfer in a square enclosure," *Trans. ASME. C. J. Heat and Mass Transfer*, **107**, No. 1, 139–146 (1985).
12. D. W. Larson and R. Viskanta, "Transient combined laminar free convection and radiation in a rectangular enclosure," *J. Fluid Mech.*, **78**, Pt. 1, 65–85 (1976).
13. W. Koutsoheras and W. W. S. Charters, "Natural convection phenomena in inclined cells with finite walls — a numerical solution," *Solar Energy*, **19**, No. 5, 433–438 (1977).
14. B. A. Meyer, J. W. Mitchell, and M. M. El-Wakil, "The effect of thermal wall properties on natural convection in inclined rectangular cells," *Trans. ASME. C. J. Heat and Mass Transfer*, **104**, No. 1, 111–117 (1982).
15. D. M. Kim and R. Viskanta, "Heat transfer by combined wall conduction and natural convection through a rectangular solid with a cavity," in: *Proc. ASME/JSME Joint Thermal Engineering Conf.*, Vol. 1, New York (1983), pp. 313–322.
16. J. Jaluria, *Natural Convection: Heat and Mass Transfer*, Pergamon Press, Oxford (1980).
17. Yu. A. Sokovishin and O. G. Martynenko, *Introduction to the Theory of Free-Convection Heat Transfer*, [in Russian], Leningrad University Press, Leningrad (1982).
18. V. I. Polezhaev, A. V. Bune, N. A. Verezub et al., *Mathematical Simulation of Convection Heat- and Mass-Transfer on the Basis of the Navier-Stokes equations* [in Russian], Nauka, Moscow (1987).

19. E. L. Tarunin, *Computational Experiment in Problems of Natural Convection* [in Russian], Izd-vo Irkutsk. Univ., Irkutsk (1990).
20. B. M. Berkovskii and V. K. Polevikov, *Computational Experiment in Convection* [in Russian], University Press, Minsk (1988).
21. B. M. Berkovskii and V. K. Polevikov, "Effect of the Prandtl number on structure and heat transfer under natural convection," *Inzh.-Fiz. Zh.*, **24**, No. 5, 842–849 (1973).
22. A. V. Lykov, *Heat Conduction Theory* [in Russian], Vyssh. Shkola, Moscow (1967).
23. G. V. Kuznetsov and M. A. Sheremet, "Simulation of three-dimensional heat transfer in an enclosure with local concentrated heat-release sources," *Izv. Tomsk. Politekh. Univer.*, **306**, No. 6, 69–72 (2003).
24. A. A. Samarskii, *Theory of Finite-Difference Schemes* [in Russian], Nauka, Moscow (1977).
25. V. M. Paskonov, V. I. Polezhaev, and L. A. Chudov, *Numerical Simulation of Heat- and Mass-Transfer Processes* [in Russian], Nauka, Moscow (1984).
26. J. Douglas, "On the numerical integration of D2u − Dx2 + D2u − Dy2 = Du − Dt by implicit methods," *J. Soc. Industr. and Appl. Math.* **3**, No. 1, 42–65 (1955).
27. D. W. Peaceman and H. H. Rachford, "The numerical solution of parabolic and elliptic differential equations," *J. Soc. Industr. and Appl. Math.* **3**, No. 1, 28–41 (1955).